

Uncertainty Quantification of Granular Computing-neural Network Model for Prediction of Pollutant Longitudinal Dispersion Coefficient in Aquatic Streams

Behzad Ghiasi

University of Tehran

Sun Yuanbin

Hohai University

Roohollah Noori (✉ roohollahnoori@gmail.com)

Iran University of Science and Technology

Hossein Sheikhan

University of Tehran

Amin Zeynolabedin

University of Tehran

Changhyun Jun

Chung-Ang University

Mohamed Hamouda

National Water Center, United Arab Emirates University

Sayed M. Bateni

University of Hawaii at Manoa

Soroush Abolfathi

University of Warwick

Research Article

Keywords: Granular Computing, Prediction of Pollutant, Aquatic Streams

Posted Date: November 10th, 2021

DOI: <https://doi.org/10.21203/rs.3.rs-1036627/v1>

License:  This work is licensed under a Creative Commons Attribution 4.0 International License.

[Read Full License](#)

Version of Record: A version of this preprint was published at Scientific Reports on March 17th, 2022. See the published version at <https://doi.org/10.1038/s41598-022-08417-4>.

1 Uncertainty quantification of granular computing-neural
2 network model for prediction of pollutant longitudinal
3 dispersion coefficient in aquatic streams

4 Behzad Ghiasi^{1,†}, Sun Yuanbin², Roohollah Noori^{3,*}, Hossein Sheikhian^{4,†}, Amin
5 Zeynolabedin⁵, Changhyun Jun⁶, Mohamed Hamouda⁷, Sayed M. Bateni⁸, and
6 Soroush Abolfathi⁹

7 ¹School of Environment, College of Engineering, University of Tehran, Tehran, 1417853111, Iran.

8 ²College of Hydrology and Water Resources, Hohai University, Nanjing, 210098, China.

9 ³School of Civil Engineering, Iran University of Science and Technology, Narmak, Tehran, 1684613114,
10 Iran.

11 ⁴Department of Geospatial Information Systems, College of Engineering, University of Tehran, Tehran,
12 1439957131, Iran.

13 ⁵School of Civil Engineering, College of Engineering, University of Tehran, Tehran, 1417613131, Iran.

14 ⁶Department of Civil and Environmental Engineering, College of Engineering, Chung-Ang University,
15 Seoul, 06974, Korea.

16 ⁷Civil and Environmental Engineering and the National Water Center, United Arab Emirates University,
17 Al Ain 15551, Abu Dhabi, United Arab Emirates.

18 ⁸Department of Civil and Environmental Engineering and Water Resources Research Center, University
19 of Hawaii at Manoa, Honolulu, HI 96822, USA.

20 ⁹School of Engineering, University of Warwick, Coventry, CV4 7AL, UK.

21 *roohollahnoori@gmail.com

22 †These authors contributed equally to this work

23 **Abstract**

24 Discharge of pollution loads into natural water systems remains a global challenge that threatens
25 water/food supply as well as endangers ecosystem services. Natural rehabilitation of the polluted streams
26 is mainly influenced by the rate of longitudinal dispersion (D_x), a key parameter with large temporal and
27 spatial fluctuates that characterizes pollution transport. The large uncertainty in estimation of D_x in
28 streams limits evaluation of water quality in natural streams and design of water quality enhancement
29 strategies. This study develops a sophisticated model coupled with granular computing and neural
30 network models (GrC-ANN) to provide robust prediction of D_x and its uncertainty for different flow-
31 geometric conditions with high spatiotemporal variability. Uncertainty analysis of D_x GrC-ANN model
32 was based on the alteration of training data fed to tune the model. Modified bootstrap method was
33 employed to generate different training patterns through resampling from a 503 global database of tracer
34 experiments in streams. Comparison between the D_x values estimated by GrC-ANN to those determined
35 from tracer measurements show the appropriateness and robustness of the proposed method in
36 determining the rate of longitudinal dispersion. GrC-ANN model with the narrowest bandwidth of

37 estimated uncertainty (bandwidth-factor =0.56) that brackets the most percentage of true D_x data (i.e.,
38 100%) is the best model to compute D_x in streams. Given considerable inherent uncertainty reported in
39 other D_x models, the D_x GrC-ANN model is suggested as a proper tool for further studies of pollutant
40 mixing in turbulent flow systems such as streams.

41 Introduction

42 Discharge of pollution loads into streams (i.e. rivers, manmade channels, and laboratory flumes) threatens
43 water/food supply for mankind and aquatic biodiversity at a global scale^{1,2}. The natural rehabilitation of
44 polluted streams is mainly characterized by the rate of longitudinal dispersion (D_x or K_x), a key parameter
45 in river water quality models with large temporal and spatial fluctuates. A challenging task in the study of
46 the pollutant fate and transport in turbulent flow systems (e.g., streams) is determining D_x for numerical
47 and analytical water quality models^{3,4}. This is because D_x is the most predominant factor influencing the
48 pollutant concentration at downstream of the point of accidental pollution^{5,8}. Starting from the late 1960s,
49 the mechanism of D_x determination in streams was introduced by Fischer⁹. From this, Fischer¹⁰ proposed
50 an analytical formula to estimate D_x that required the full and detailed knowledge of the flow-geometric
51 conditions of the system under study.

52 Given that the flow-geometric data for streams are highly variable in temporal and spatial scales,
53 such data are not readily measured and available. Also, the complex numerical procedures required to
54 solve Fischer¹⁰ equation, have led to several simplifications to determine D_x . Hence, the predictions of D_x
55 from the simplified models often deviate from the field-estimated measurements up to several orders of
56 magnitude^{11,12}. These simplifications are mainly exclusion of some difficult accessible variables such as
57 flow-geometric irregularities that influence dispersion mechanism in streams. Although in many cases the
58 impact of the excluded variables is somewhat embedded in other variables used in D_x estimation models,
59 they do not fully represent the complex interactions between the absent variables and D_x . For example,
60 friction term (i.e., rate of flow velocity to shear velocity – U/U^*), as a simply accessible input for D_x
61 estimation models, to some extent can represent the impact of lateral and vertical irregularities in streams
62 that affect the rate of dispersion¹³. However, these irregularities produce shear flows and secondary
63 currents that can alternate the D_x . Simultaneously, the former causes an increase in D_x whilst the latter
64 decreases D_x ^{8,14-18}. The complex interactions between the flow-geometric data and dispersion mechanism
65 prohibit reaching an accurate estimation of D_x in streams whilst some effective variables on dispersion
66 mechanism are excluded (e.g., stream bed shape factor and sinuosity).

67 In recent decades, and with the advancement in artificial intelligence (AI) models, they became
68 powerful tools to solve complex engineering problems¹⁹⁻²⁹. A number of AI-based studies have conducted
69 to enhance the accuracy of D_x estimation in turbulent flow systems such as streams^{30,33}. Given that AI
70 techniques are able to map the complex non-linear input-output relationships even when some important
71 information are missing³⁴, their applications in estimating the D_x have been investigated by several
72 studies^{30,33,35-44}. However, complex nature of dispersion mechanism in turbulent flow systems with
73 variations in both spatial and temporal scales, as well as the inevitable simplification assumptions that are
74 needed for modelling will result in uncertainty of D_x using AI models. In a study conducted by Noori et
75 al.⁴⁵, they reported that although the AI techniques outperform traditional empirical models for estimation
76 of D_x , they are still subjected to uncertainty induced by changes in their training patterns. The inaccuracy
77 in estimation of the D_x using AI models can limit water quality assessment and design of appropriate
78 measures to improve the water quality of aquatic flows. Hence, developing robust methodological
79 framework to quantify the prediction uncertainty of the D_x from AI models is essential for developing
80 appropriate AI-based water quality models.

81 Granular computing (GrC) model is a highly efficient AI-based model which has recently shown an
82 excellent potential to solve complex problems in engineering community^{42,46,47}. GrC model is a novel tool

83 capable of applying the granules in the process of nonlinear problem solving⁴⁸. In the GrC model, the
84 natural rules between the data are extracted by means of the rule mining algorithm, operating on a set of
85 information arranged as information table. The granule measures involved in the process of information
86 mining, has made GrC as a powerful tool to map a set of inputs to a set of outputs in different fields of
87 science and engineering^{49,50}.

88 However, similar to other AI models, the GrC performance can be adversely influenced by the
89 selection of training patterns. Therefore, the effects of changes in training patterns on the performance of
90 GrC model should be investigated, to understand and quantify the degree of uncertainty in the model's
91 prediction of D_x in water quality assessments. In this study, we first replaced an artificial neural network
92 (ANN) with rules' information in the GrC to improve its performance (GrC-ANN). Then, we developed a
93 D_x estimation model using GrC-ANN model. Finally, a comprehensive uncertainty analysis method was
94 proposed for the model-estimated D_x in streams, to compare the accuracy of D_x predicted by GrC-ANN
95 with other AI-based D_x models in the literature.

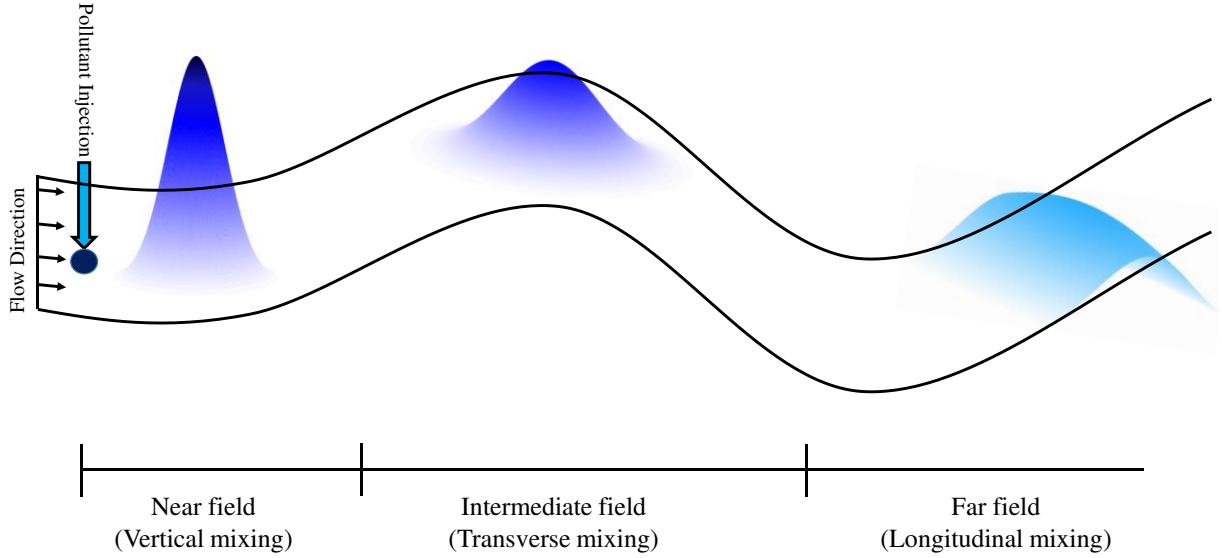
96 By considering the above, this study, for the first time, highlights the application, strengthens and
97 weaknesses of GrC-ANN model in the field of hydrological and water quality engineering. More
98 importantly, this study introduces a framework for uncertainty determination of the GrC-ANN model, a
99 subject with no documentation in literature, that is beneficial for reliable application of this model in
100 water-environmental community and other fields of science/engineering.

101 Methods

102 **Longitudinal dispersion.** Non-reactive pollutant mixing process in aquatic systems is a complex three-
103 dimensional (3-D) flow process, consists of molecular and turbulent diffusion, and shear dispersion
104 (simply referred to "dispersion") mechanism where the latter is the net trace of velocity shear over the
105 flow width and depth, and the turbulent mixing¹¹. In the natural streams that are specifically much longer
106 than width or depth of the flow, the pollutants become well-mixed in the vertical and transverse directions
107 rather than the longitudinal mixing (Fig. 1). Therefore, pollutant fate and transport in streams is usually
108 studied by the application of 1-D dispersion model quantified by the advection-dispersion equation, i.e.,
109 Eq. (1)^{51,52}.

$$110 \quad \frac{\partial C}{\partial t} + U \frac{\partial C}{\partial x} = D_x \frac{\partial^2 C}{\partial x^2} \quad (1)$$

111 In Eq. (1), C and U , are the average cross-sectional concentration and average longitudinal velocity,
112 respectively; t and x are time and longitudinal coordinate in the stream-wise direction, respectively.



113

114 **Figure 1.** Schematic view of pollutant mixing in streams (adapted from Kilpatrick and Wilson⁵³).

115 Ideally, vertical and (transverse) dispersion in streams takes place close to (in intermediate fields
 116 from) the pollutant discharge location, whilst the longitudinal dispersion occurs far from the point of
 117 pollutant discharge where solute become readily well-mixed in both vertical and transverse directions
 118 (Fig. 1). In streams, the longitudinal dispersion usually varies from 10^{-1} to 10^7 m^2/s ^{10,13,54,55} and the
 119 diffusion coefficient ranges from 10^{-9} (molecular) to 10^{-2} m^2/s (turbulent)⁵. Therefore, dispersion is the
 120 dominant mechanism of mixing process, by several orders of magnitude⁵⁶, highlighting the necessity of
 121 developing robust methodological approach to quantify the dispersion and mixing coefficient in the
 122 streams.

123 **D_x parametrization.** Pioneering work on quantification of dispersion mechanism in pipes date back to
 124 Taylor's studies^{57,58}. Thereafter, Taylor's approach was used for quantifying dispersion in streams with
 125 the assumption of no limits for the width of the channel⁵⁹. However, the Elder's formula underestimates
 126 the dispersion in natural streams since it does not consider the lateral velocity shear^{10,60}. In streams, the
 127 lateral velocity shear mechanism plays a more dominant role in determining the mixing compared to the
 128 vertical shear. On this basis, Fischer⁹ derived an analytical formula for determining D_x :

$$129 \quad D_x = \left\{ \int_0^W h(y) \dot{u}(y) \int_0^y [1/\varepsilon_t(y) h(y)] \int_0^y h(y) \dot{u}(y) dy dy dy \right\} / A \quad (2)$$

130 where, W denotes the local flow width, x is the longitudinal coordinate, y is the lateral coordinate, $\dot{u}(y)$ is
 131 the local velocity deviation, $h(y)$ represents the local flow depth, $\varepsilon_t(y)$ is local lateral mixing coefficient,
 132 and A represents the local flow cross-sectional area.

133 In Eq. (2), the flow is supposed to be 1-D, i.e., the pollutant is mixed in both vertical and lateral
 134 directions well, a condition that is rarely satisfied in turbulent flow systems such as natural streams and
 135 even in laboratory flumes due to existence of secondary currents⁶¹. Also, Fischer⁹ equation has been
 136 derived based on the assumption that the dispersion is controlled by lateral shear rather than vertical
 137 shear, a condition that may not satisfy well for the narrow and deep rivers where aspect ratio (i.e., river
 138 flow width to depth – W/H) is small⁵. Such drawbacks of Eq. (2) lead to inaccurate estimation of D_x
 139 compared to those values determined from tracer experiments. The deviation between D_x values estimated
 140 by Eq. (2) and those true values is maximum for the case of non-uniform flow in real streams, although
 141 Fischer⁹ model can well approximate the dispersion for the case of uniform flow⁶². In addition to the
 142 inherent drawbacks in practical application of the Eq. (2), it also requires detailed information on the

143 geometrical properties (i.e. cross-section, bathymetry) of stream, as well as the lateral flow velocity
144 profiles. Collecting such information is rather costly and time consuming, and often requires very detailed
145 flow measurements which are not readily available. Therefore, practical application of Fischer⁹ model is
146 limited.

147 To address the difficulties in using Eq. (2), Fischer⁶³ suggested a simplified empirical equation that
148 correlated D_x with pertinent dimensionless variables of W/H and U/U^* (Eq. (3)).

$$149 \frac{D_x}{HU^*} = a \left(\frac{W}{H} \right)^b \left(\frac{U}{U^*} \right)^c \quad (3)$$

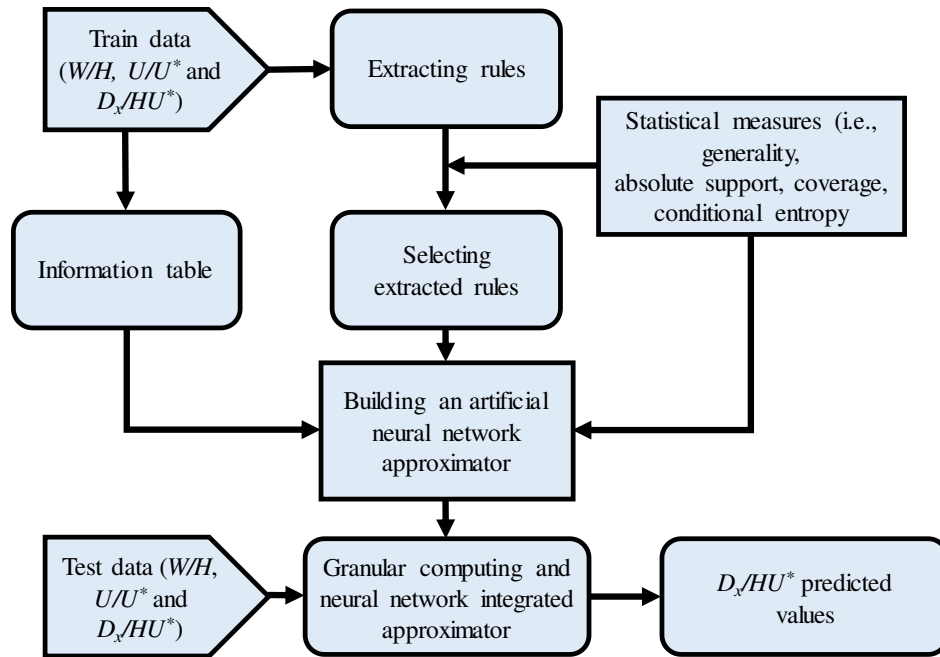
150 Fischer⁶³ modified formula for determining the dispersion coefficient (Eq. (3)), has been widely
151 used and validated by other researchers and rely on parameters which can be practically determined.

152 **Data collection.** This study aims to estimate D_x in streams using GrC-ANN model. In this regard, a
153 global tracer database consisting of 503 observations from natural streams and laboratory flumes was
154 used to develop the model and validate the performance of the proposed GrC-ANN model. This database
155 was compiled by Riahi-Madvar et al.⁶⁴, consisting of a comprehensive range of flow conditions, stream
156 geometrical properties, and pollution loading. It should be noted that although the database used in this
157 study is more comprehensive compared to other studies on D_x estimation, it does not fully include high
158 extreme values of D_x ¹².

159 **GrC-ANN development.** In-depth description and model development for the GrC and GrC-ANN
160 approach for environmental pollution modelling were given in Noori et al.⁴² and Ghiasi et al.⁴⁶,
161 respectively. and detailed information about these models documented by Sheikhian et al.^{47,48} conducted
162 comprehensive review of the models and their performance. Hence, we shortened the descriptions of
163 GrC-ANN model developed in this study.

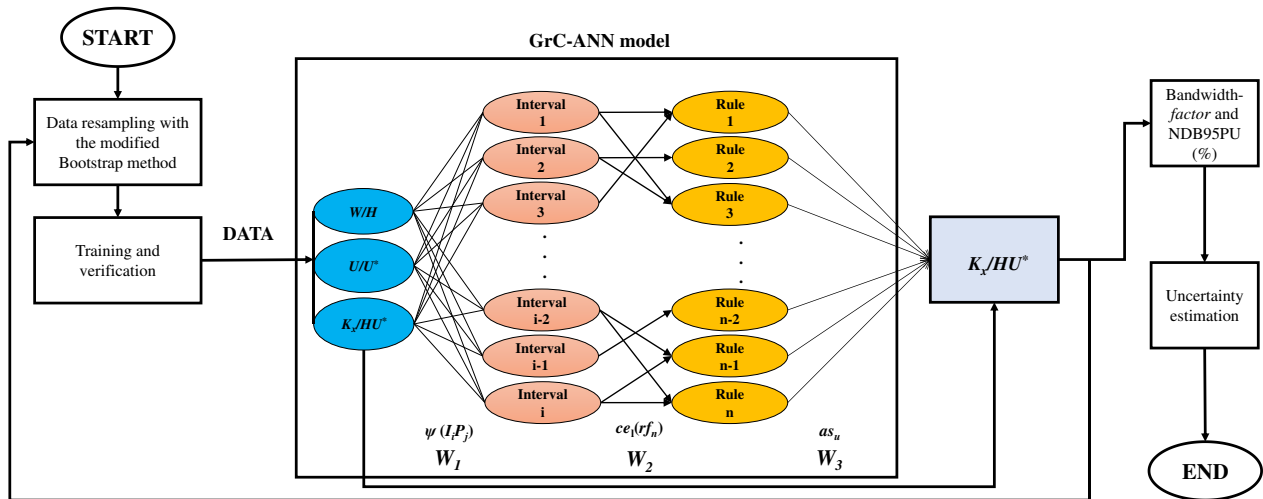
164 The GrC applies different measures to construct the high-quality classification rules in the form of
165 IF-THEN statements⁶⁵. In this study, GrC extracts the rules from the global tracer database consisting of
166 503 observations from natural streams and laboratory flumes based on conditional entropy (CE) and
167 absolute support (AS) so that rules with the minimum CE value and the maximum AS are extracted from
168 the database. To form a granular decision tree, the priority of rules in the tree is determined based on
169 higher generality (G) and coverage (CV).

170 A basic GrC model has two major deficiencies. First, it prioritizes rules based on their obtained
171 parameters and uses the first rule satisfied by input data to define its output^{66,67}. Second, after
172 classification, some of the input patterns may remain unclassified if they do not meet the requirements of
173 the classification rule set. Hence, the GrC-ANN model proposed in this study uses an integration of GrC
174 rule generation and ANN model (Fig. 2). The proposed modelling approach benefiting the information
175 gathered from existing relationship among extracted rules from GrC algorithm, by applying a group of
176 rules providing information about the input pattern of data (i.e., W/H , U/U^* and D_x/HU^*), ranked by the
177 rule relevance measurements undertaken by the GrC. This approach allows the model to use the
178 mentioned rule quality parameters to construct the approximator structure, instead of common time-
179 consuming iterative learning procedure⁴⁶.



180
181 **Figure 2.** Procedure of integrating GrC and ANN for determining longitudinal dispersion coefficient.

182 The GrC-ANN structure proposed in this paper comprises layers as a conventional neural network
183 including the input layer, two computing layers, and the output (aggregation) layer (Fig. 3). The layers are
184 customized to support the proposed idea. The input layer contains nodes equal to attributes of the data
185 records (i.e., W/H , U/U^* , and D_x/HU^*). Computing layers comprise from two inner-connected layers
186 including pattern layer and rule firing layer. These layers within the computing layer, receive values that
187 are valid according to the criteria presented in the input layer. The third layer contains the set of qualified
188 extracted rules by GrC-ANN and embeds the classification rules. The aggregation layer assigns an output
189 value to the input pattern of the data. The connection weights of the rule-firing layer and the aggregation
190 layer are given by the statistical measure of absolute support provided by the corresponding rule to its
191 output value, to consider the accuracy of the rules in determining that output value.



192
193 **Figure 3.** Schematic of the GrC-ANN modelling details of this study.

194 **Uncertainty determination.** Similar to other data-driven models, the GrC-ANN model minimizes the
 195 error function based on the fed data with the aid of a supervised algorithm throughout the training
 196 process⁴⁹. Hence, training plays a vital role in quantification of the model’s uncertainty caused by
 197 different tuning sets. In this study, the GrC-ANN model was tuned to map inputs W/H and U/U^* to target
 198 D_x/HU^* based on finite training patterns resampled from 503 observations of the global tracer database.
 199 Probabilistically, each training pattern used for tuning the GrC-ANN model is different from others
 200 resampled from the global database of tracer experiments. Thus, each training pattern could produce
 201 different set of GrC-ANN parameters as well as different outputs for estimation of D_x/HU^* .

202 The modified bootstrap method suggested by Noori et al.¹² was used to resample distinct training
 203 patterns for tuning D_x/HU^* GrC-ANN model. This method ensures that the chosen training patterns are
 204 fully representative of the statistical characteristics of the 503 tracer experiments of the global database
 205 used in this study. This is important since the global database used in this study rarely has large D_x
 206 instances¹², denoting that these large dispersion values are likely under-represented in the training patterns
 207 chosen by the traditional bootstrap technique. This issue can result in poor training of D_x/HU^* GrC-ANN
 208 model and consequently increase the model’s uncertainty. Detailed description on the bootstrap method is
 209 given by Efron and Tibshirani⁶⁸, while Noori et al.¹² modified the bootstrap method.

210 However, we used different outputs of the D_x/HU^* GrC-ANN model in verification stage, resulted
 211 from the change in the training patterns, as a measure of the model’s uncertainty⁶⁹. We computed an
 212 interval band of the GrC-ANN estimations of D_x/HU^* with a level of significant of 95%. Then, two
 213 measures were used to assess variations in the different responses of the D_x/HU^* GrC-ANN model in
 214 verification stage including bandwidth-*factor* and the number of bracketed D_x/HU^* data using 95% of
 215 predicted uncertainties (NBD95PU) as shown in Eqs. (4) and (5), respectively⁷⁰. Given these two
 216 measures, the uncertainty in estimation of the D_x/HU^* GrC-ANN model in verification stage was
 217 quantified.

$$218 \text{ bandwidth-}factor = \left\{ \left(\frac{1}{n} \right) \sum_{i=1}^n (X_U - X_L) \right\} / \sigma_x \quad (4)$$

$$219 \text{ NBD95PU (\%)} = (1/n) \text{count}\{Q | (X_L \leq Q \leq X_U)\} \quad (5)$$

220 where σ_x is the standard deviation of the target D_x/HU^* , and X_U and X_L are the maximum and minimum
 221 of the estimated D_x/HU^* for each training pattern, respectively.

222 **Figure 3** illustrates a detailed description of the model development and uncertainty quantification
 223 process proposed for this study.

224 3. Results and discussion

225 **Tuned GrC-ANN models.** The correlation among W , H , U , U^* and D_x is shown in Fig. 4A. The
 226 correlation coefficients for the model variables in dimensionless format, i.e. W/H , U/U^* and D_x/HU^* and
 227 the corresponding statistical significance level are illustrated in Fig. 4B. In dimensional form, D_x/HU^* is
 228 more correlated with the geometrical configuration W/H of the stream (correlation coefficient =0.21, p -
 229 value <0.1) than the flow characteristic U/U^* (correlation coefficient =0.002, p -value >0.1), which
 230 confirm the results reported by Noori et al.¹².

231
 232
 233

| | | | | |
|-----------------------------|-----------------------------|-----------------------------|-----------------------------|-----------------------------|
| W | 0.72 (p -value <0.01) | 0.15 (p -value <0.01) | 0.00 (p -value >0.1) | 0.18 (p -value <0.01) |
| 0.72 (p -value <0.01) | H | 0.08 (p -value <0.01) | 0.00 (p -value >0.1) | 0.11 (p -value <0.01) |
| 0.15 (p -value <0.01) | 0.08 (p -value <0.01) | U | 0.07 (p -value <0.01) | 0.22 (p -value <0.01) |
| 0.00 (p -value >0.1) | 0.00 (p -value >0.1) | 0.07 (p -value <0.01) | U^* | 0.03 (p -value <0.01) |
| 0.18 (p -value <0.01) | 0.11 (p -value <0.01) | 0.22 (p -value <0.01) | 0.03 (p -value <0.01) | D_x |

234

(A)

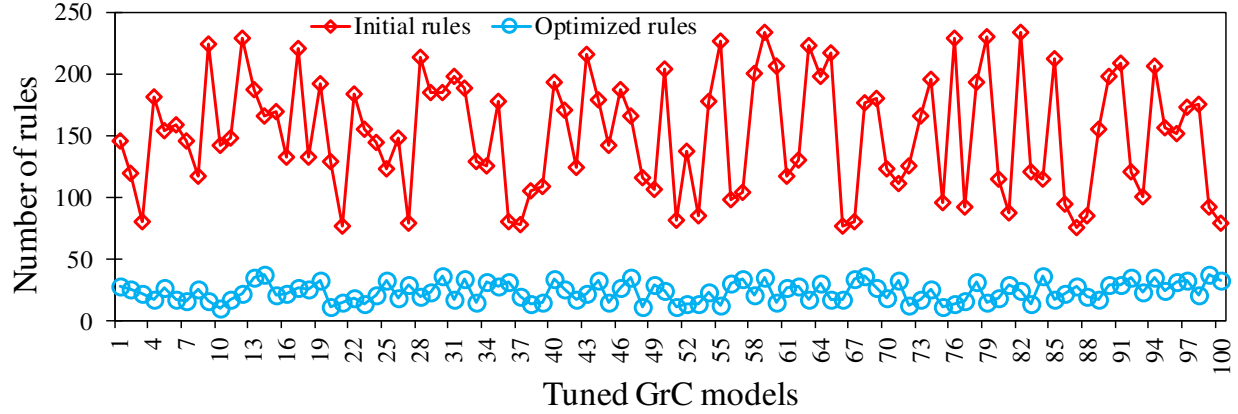
| | | |
|-----------------------------|-----------------------------|-----------------------------|
| W/H | 0.002 (p -value >0.1) | 0.21 (p -value <0.01) |
| 0.002 (p -value >0.1) | U/U^* | 0.01 (p -value >0.1) |
| 0.21 (p -value <0.01) | 0.01 (p -value >0.1) | D_x/HU^* |

235

(B)

236 **Figure 4.** The correlation coefficient plots of (A) W , H , U , U^* , and D_x , (B) W/H , U/U^* and D_x/HU^* .

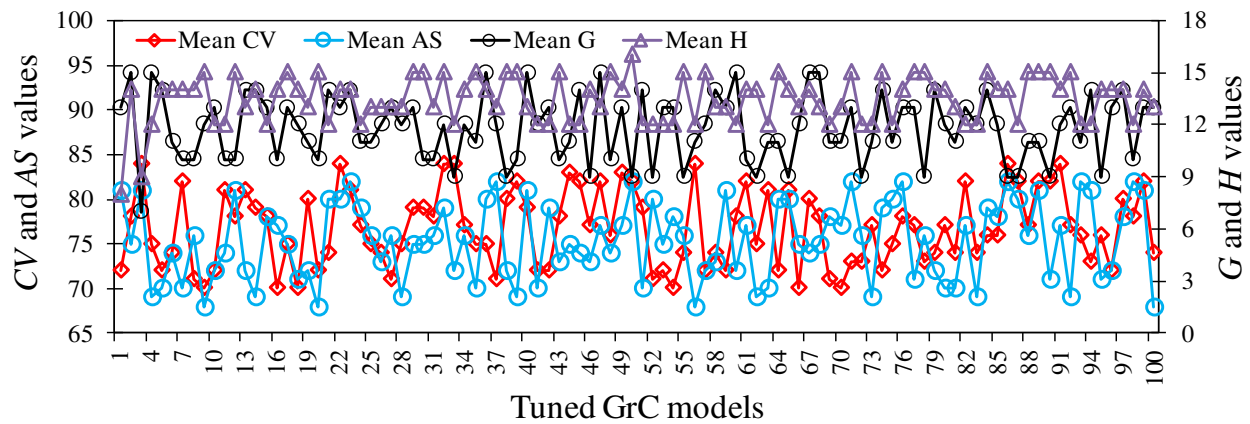
237 To apply the GrC-ANN model, the 503 observations from real streams and laboratory flumes were
 238 scaled between 0 and 1. 40 data were excluded away from the 503 observations of global tracer
 239 experiments for the model verification. Then, 100 distinct training patterns were randomly resampled
 240 from the remaining database, i.e. 463 observations, with replacement to tune 100 different D_x/HU^* GrC-
 241 ANN models. Each training pattern consists of 80 data, and the 40 pre-assigned verification data. The
 242 model inputs include, aspect ratio and friction term, and dimensionless target D_x/HU^* were clustered
 243 based on their indiscernibility in the given attributes. To form final rule network, the GrC-based rule
 244 extraction algorithm was used to select the best granules of information by considering the measurements
 245 CE , AS , G , and CV computed for each rule. In this regard, AS and CE indices were employed to extract
 246 the set of possible valid rules by considering minimum and maximum threshold values of 0.75 and 0.5 for
 247 these parameters, respectively, in accordance to the similar studies in the literature^{42,71,72}. At this stage, if a
 248 rule caused redundancy in the rule set, it was considered as an active granule and was replaced with a
 249 granule that had more consistency in the set of rules. Using the proposed methodology led to extraction of
 250 a range of rules, varied from 76 to 234, for tuning the GrC models based on the training patterns (Fig.
 251 5A).



252

253

(A)



254

255

(B)

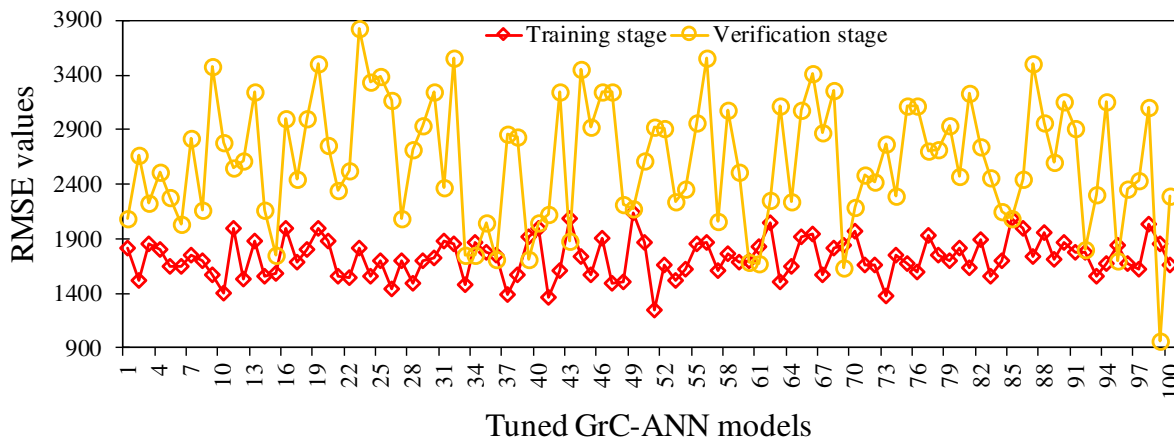
256 **Figure 5.** (A) Number of initial and optimized rules, and (B) the mean values of quality indices for the
 257 final rules for each tuned GrC models.

258 In the next step, the *CV* and *G* indices were applied to prioritize the rules resulted in the final rule
 259 sets. The optimized rules varied from 10 to 38 for the models tuned based on the training patterns (Fig.
 260 5A). The mean values of quality indices for the final rules selected for each tuned model are illustrated in
 261 Fig. 5B. According to Fig. 5B, the *G* values ranged between 0 and 0.4 indicating the rules' generality
 262 does not pertain to big values of *G*, which confirms the results of previous GrC modelling studies^{42,66}. The
 263 *CV* varied between 0 and 1, pertaining to the numbers of extracted rules by each class and dataset covered
 264 by each rule, following Yao and Yao⁶⁶ suggestion.

265 100 optimized rule sets computed correspond to one hundred distinct training patterns are then fed
 266 to the GrC-ANN modelling structure. In this regard, the rule quality indices were embedded into an ANN
 267 structure instead of initial weights, forming a GrC-ANN model corresponding to each optimized rule set.
 268 The best network structures describing the relations between the inputs (W/H and U/U^*) and the output
 269 (D_x/HU^*) data were determined based on the quality index of root mean square error (RMSE) for each
 270 GrC-ANN model tuned by the distinct training patterns (Fig. 6A). Analysis of the results show the RMSE
 271 values for the tuned D_x/HU^* GrC-ANN models, in training and verification stages varied from 1251 to
 272 2142 and 966 to 3826, respectively (Fig. 6A).

273 Figure 7 shows the difference between the true (field-estimated) D_x/HU^* values and those
 274 predicted by each tuned D_x/HU^* GrC-ANN model. The minimum (i.e., -10934) and the maximum (i.e.,
 275 7471) errors were produced in D_x/HU^* GrC-ANN models #42 and #100, respectively. In general, the

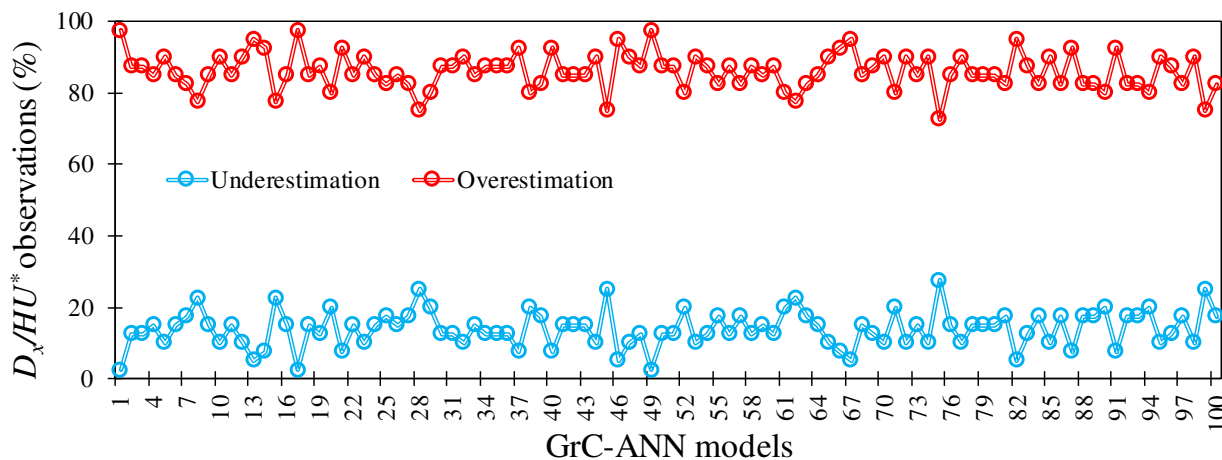
276 GrC-ANN models overestimate the D_x/HU^* values for around 86% of observations (Fig. 6B). Such
 277 overestimation of D_x was reported by Etemad-Shahidi and Taghipour⁷³ for the D_x models proposed by
 278 Liu⁵⁵, Seo and Cheong¹³, Deng et al.⁵¹, and Sahay and Dutta⁷⁴. However, using the overestimated
 279 D_x/HU^* values in corporation with 1-D ADE models give lower maximum concentration rate at
 280 locations which are far from the pollutant injection point¹². Therefore, the tuned D_x/HU^* GrC-ANN
 281 model must be used with caution in hydro-environmental studies such as outfall design and/or risk
 282 assessment researches from accidental hazardous pollution.



283

(A)

284

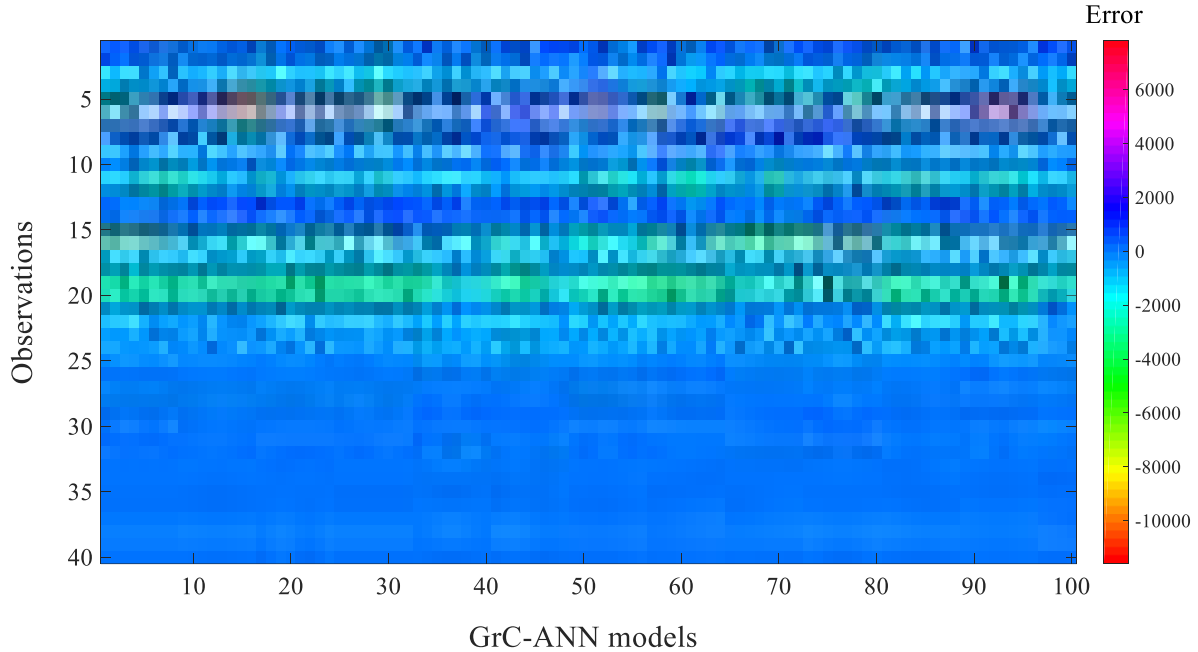


(B)

285

286

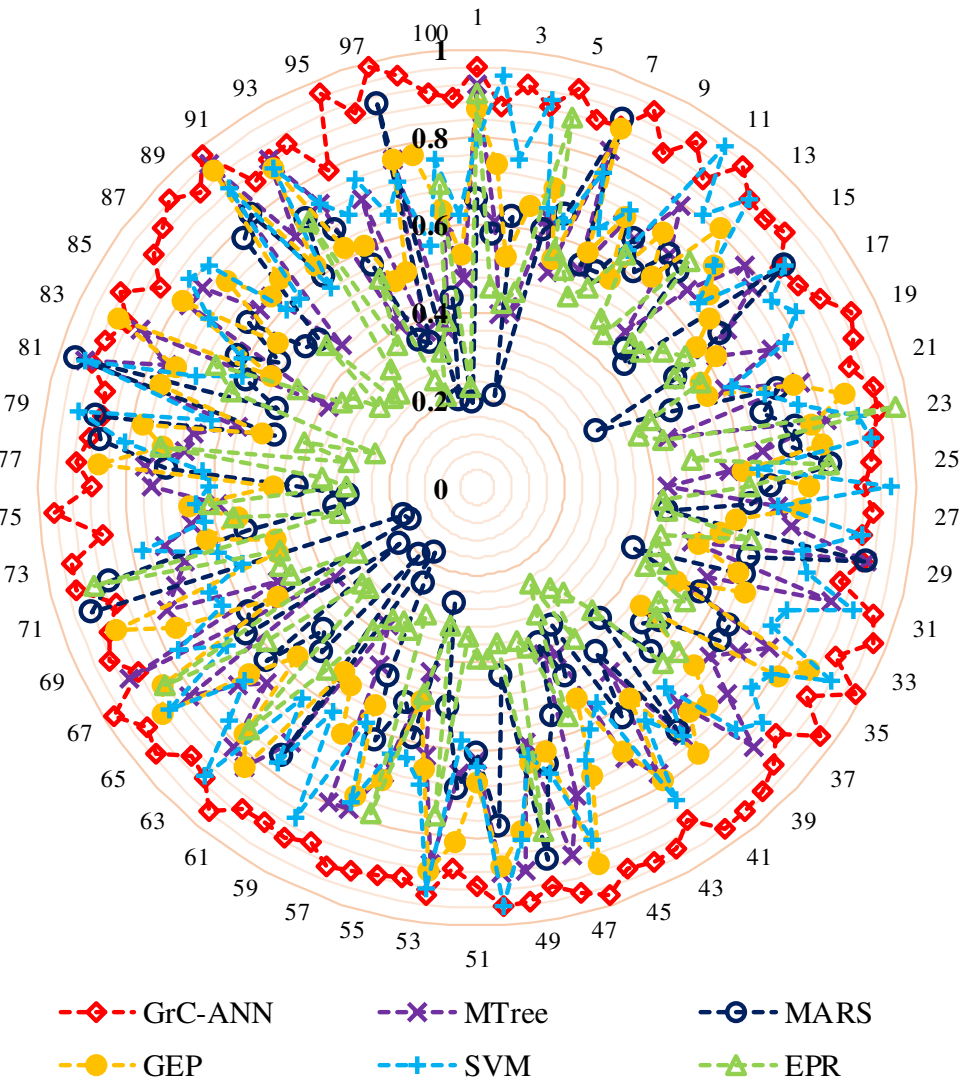
287 **Figure 6.** (A) Root mean square error (RMSE) values calculated for the tuned D_x/HU^* GrC-ANN
 288 models in training and verification stages, and (B) D_x/HU^* observations (%) with underestimation and
 289 overestimation in GrC-ANN models tuned by the distinct training patterns.



290

291 **Figure 7.** Difference between the true D_x/HU^* values and those predicted using GrC-ANN models tuned
 292 by the distinct training patterns.

293 The GrC prioritizes rules based upon their obtained parameters and uses the first rule satisfied by
 294 aspect ratio and friction term data to define dimensionless term D_x/HU^* as the model output. In addition,
 295 some of the input patterns may remain unclassified if they do not meet the requirements of the
 296 classification rule set in the GrC model⁶⁷. Meanwhile, GrC-ANN uses the final rule set selected by GrC
 297 instead of the initial weights⁴⁶. In other words, a conventional ANN model provides results which is
 298 influenced by initial weights generated in a random manner, yielding to different results from the same set
 299 of training information. In addition, the proposed D_x/HU^* GrC-ANN model replaces the learning part of
 300 the ANN with the information from rule quality measures and ensures that no connection or node are
 301 remained without a transparent description. The GrC-ANN modelling approach described in the present
 302 study is a significant improvement to the conventional ANN modelling approaches which contain hidden
 303 neurons obtaining their connection weights by learning through a black-box learning algorithm. Hence,
 304 the tuned D_x/HU^* GrC-ANN theoretically provide a more robust framework than both GrC and ANN
 305 models. Previous studies also confirmed the performance superiority of GrC compared to ANN and
 306 adaptive neuro fuzzy inference system (ANFIS) developed for D_x/HU^* predictions (e.g., Ghiasi et al.⁴⁶).
 307 Comparative analysis of the tuned GrC-ANN models developed in this study, and other AI models
 308 including model tree (MTree), gene-expression programming (GEP), evolutionary polynomial regression
 309 (EPR), support vector machine (SVM), and multivariate adaptive regression splines (MARS), developed
 310 by Najafzadeh et al.⁷⁵, highlights that the proposed GrC-ANN models are capable of better and more
 311 robust approximation of longitudinal dispersion (D_x/HU^*) in stream (Fig. 8). As shown in Fig. 8, the
 312 determination coefficient (R^2) values determined for the GrC-ANN models in verification stage, are much
 313 larger than those reported for ERP and MARS models.

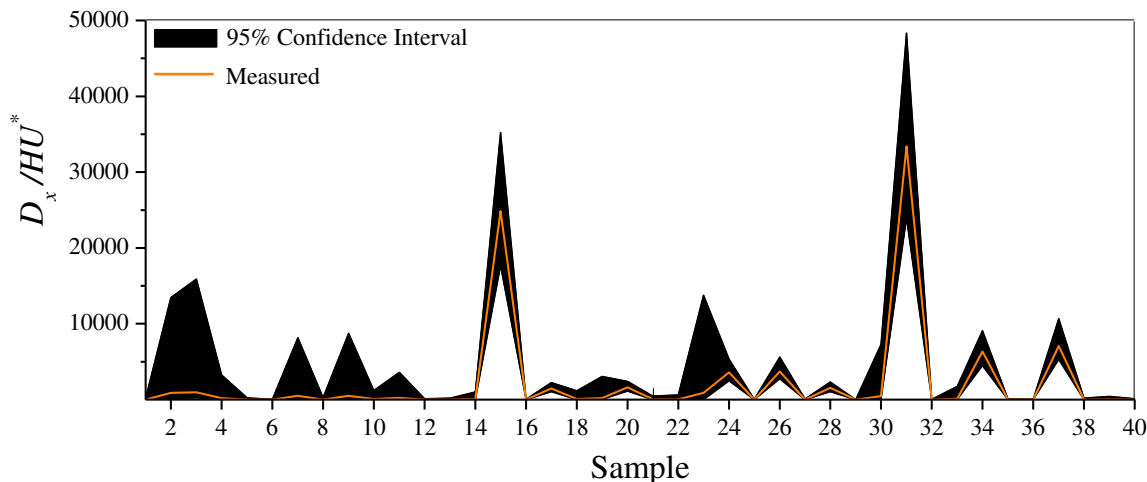


314
 315 **Figure 8.** Determination of coefficient (R^2) values calculated for D_x/HU^* prediction during the
 316 verification step of the tuned GrC-ANN models developed in this study, and those reported for model tree
 317 (MTree), gene-expression programming (GEP), evolutionary polynomial regression (EPR), support
 318 vector machine (SVM) and multivariate adaptive regression splines (MARS)) by Najafzadeh et al.⁷⁵.

319 **3.2. GrC-ANN uncertainty.** The D_x/HU^* values estimated during the verification stage by the 100 GrC-
 320 ANN models tuned under distinct training patterns were used to measure the model uncertainty. In this
 321 regard, prediction intervals corresponding to each D_x/HU^* observation was computed by considering the
 322 level of significant of 95% (Fig. 9). These prediction intervals show the deviation from the true D_x/HU^*
 323 values, denoting the uncertainty associated with the GrC-ANN predictions of longitudinal dispersion in
 324 streams.

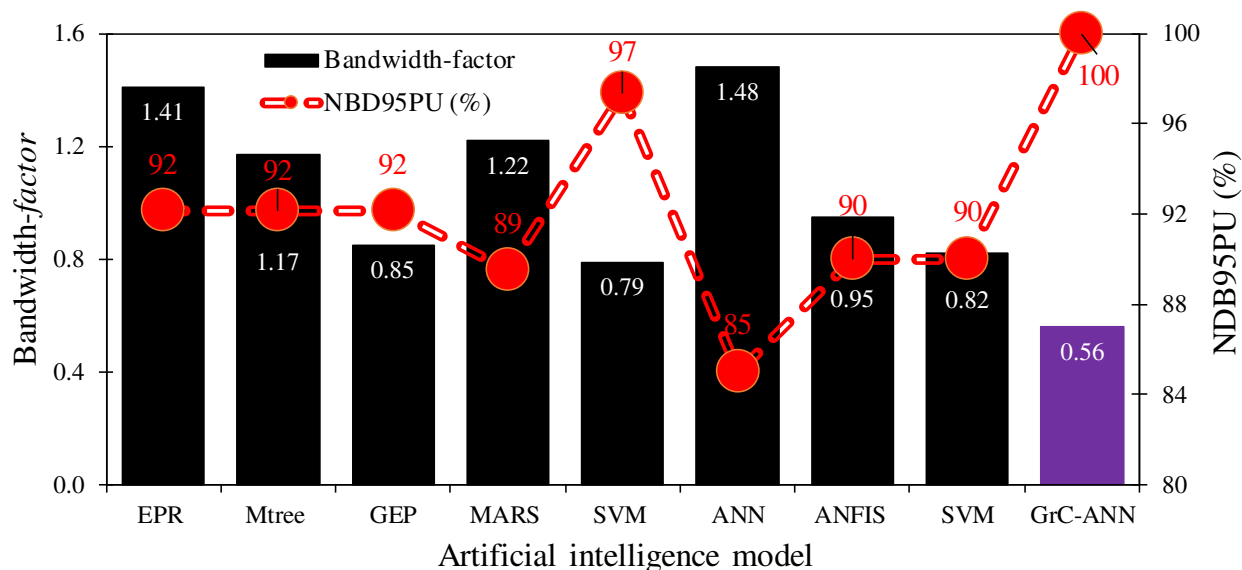
325 **Figure 9** shows that the true D_x/HU^* values are fully located between the lower and upper bands of
 326 the uncertainty, concluding the appropriate performance of the GrC-ANN model based on the NDB95PU
 327 (%) index. Also the small value of the bandwidth-factor (= 0.56) indicates the small deviation of the
 328 predicted D_x/HU^* values by the GrC-ANN models from the measured values, leading to low uncertainty
 329 of the model. **Fig. 9** shows that the proposed GrC-ANN model has good performance in predicting both
 330 large and small D_x/HU^* values with a narrow bandwidth of uncertainty, highlighting the model

331 superiority in predicting the D_x/HU^* compared to other AI models which are suffering from large
 332 uncertainty in estimation of D_x ^{12,42,45,75}.



333
 334 **Figure 9.** GrC-ANN model uncertainty for estimation of D_x/HU^* in streams.

335 However, neither the GrC-ANN model nor other mathematical and statistical models can fully
 336 understand and predict the dispersion processes in real streams. Therefore, the results illustrated in Fig. 9
 337 still contain some degree of uncertainty in the prediction of D_x/HU^* from GrC-ANN model. To compare
 338 the uncertainty of the predicted D_x/HU^* from GrC-ANN with other AI models, the bandwidth-factor
 339 and NDB95PU (%) values computed for these models are illustrated in Fig. 10. This figure shows that
 340 D_x/HU^* GrC-ANN model has the smallest bandwidth-factor value amongst the 9 AI-based models
 341 examined in this study. Also, D_x/HU^* GrC-ANN model has the largest NDB95PU (%) value compared
 342 to other AI models (i.e., EPR, MTree, GEP, SVM, MARS, ANN, and ANFIS). These measures suggest
 343 that the uncertainty in the prediction of D_x/HU^* from GrC-ANN model is far less than those reported for
 344 other well-established AI models for the case of pollutant transport in streams.



345
 346 **Figure 10.** Comparison of the bandwidth-factor and the NDB95PU (%) values of the GrC-ANN model
 347 developed in this study (i.e., D_x/HU^* GrC-ANN), with ANN and ANFIS models⁴⁵, SVM, GEP, MTree,
 348 MARS, and EPR models⁷⁵.

349 A review of the past studies indicates that the accuracy of the models suggested for estimation of D_x
350 largely varies depending on the choice of AI modelling approach and the dataset used⁷⁶. For example, the
351 accuracy of ANN model developed for estimation of D_x , measured as R^2 , varied from 0.34⁷⁶ to 0.98⁷⁷. The
352 R^2 value for the SVM model is ranging from 0.4⁷⁶ and 0.76⁷⁸. Also, ANFIS model developed for the
353 estimation of D_x in streams show an R^2 value varying from 0.50⁷⁹ to 0.96⁴⁶. The same results have also
354 been reported for traditional empirical studies where R^2 value varies from 0.36⁸⁰ to 0.96⁴². Such large
355 variations in the accuracy of D_x estimation clearly specify the importance of training patterns used to tune
356 the models for predicting the rate of longitudinal dispersion in streams, an important issue that generally
357 overlooked in the previous studies. Therefore, introducing a D_x model tuned based on a single training
358 pattern does not provide a comprehensive and robust understanding of the possible change of D_x in real
359 case studies, where D_x largely fluctuates and influenced by the irregularities in flow hydrodynamics and
360 the geometric characteristics of streams.

361 However, study of the Fig. 9 reveals that despite modified and enhanced training patterns adopted
362 in this study, there remains some uncertainty in the prediction of the D_x/HU^* from GrC-ANN model,
363 which can be considerable at times and leading to a wide confidence interval band for some samples. In
364 fact, in the D_x/HU^* GrC-ANN modelling process, some rules are eliminated due to low criteria values
365 (i.e., G , AS , CV , and CE). Therefore, the selected rules, which govern the final prediction of the model, do
366 not fully represent the complex mechanisms of the longitudinal dispersion in streams, leading to
367 inevitable uncertainty in the predictions by GrC-ANN model. In addition, diversity of streams and the
368 irregularities in geometric characteristics and nonlinearity of the flow hydrodynamics add to the
369 complexity of the mixing mechanisms in the streams. Therefore, full identification, quantification and
370 inclusion of these intricate natural processes in a mathematical or statistical model is not possible. This is
371 correct even for the non-simplified models for prediction of D_x , i.e. Eq. (2), where estimated D_x values are
372 still not in full agreement with those values measured in the field. For example, the minimum error
373 between the estimated and field-measurement of D_x values occurs for the case of a uniform flow, that is
374 usually less than 30%⁶². In the case of non-uniform flow in large meandrous streams with severe
375 irregularities in bathymetry, and spatiotemporal variations in flow hydrodynamics, the estimated D_x using
376 Eq. (2) usually deviates from the field measurements by several orders of magnitude¹¹. The problem of
377 inaccuracy in modelling predictions raises up when using Eq. (3), derived based on simplified
378 assumptions for Eq. (2), and by exclusion of important parameters influencing D_x such as S_f and
379 S_n ^{5,11,16,80,811}. These excluded parameters are seldom monitored in streams due to the difficulties associated
380 with their measurement. Another factor that contribute to the uncertainty in prediction of longitudinal
381 dispersion from GrC-ANN model is the rare presence of very large D_x values in the dataset used in this
382 study. Analysis of the dataset used in this study shows that only around 1% of the 503 global dataset of
383 tracer experiments consists of $D_x > 1000$ m²/s, whilst the maximum value of D_x in the dataset is around
384 1800 m²/s¹². This absence of very large D_x in the dataset, is leading to uncertainty in the D_x/HU^*
385 predicted by the GrC-ANN model.

386 Conclusions

387 Rate of longitudinal dispersion (D_x) dominantly influences the pollutant transport and fate in streams.
388 Given the high spatiotemporal variability of D_x , previous single-based trained models cannot robustly
389 understand the complex nonlinear interactions between the parameters that govern the longitudinal
390 dispersion in the streams and cannot capture the uncertainty associated with the predictive models for D_x
391 in streams. This provides rigorous methodological approach to examine and quantify the uncertainty in
392 the prediction of D_x/HU^* from the proposed GrC-ANN model, by studying the distinct training patterns
393 used to optimize the model's parameters. The detailed analysis of the results highlights that although
394 D_x/HU^* predicted by GrC-ANN model outperform other AI-based dispersion models, there remains

395 some uncertainty in the predicted D_x from the model which need careful consideration and evaluation.
396 This finding suggests that river water quality assessments and management studies should consider the
397 impacts of uncertainty associated with the D_x estimation on the pollutant concentrations, that could result
398 in detrimental impacts on aquatic biodiversity, and ecosystem function in streams as well as human
399 health. Enhanced data on the flow hydrodynamics and the geometric features in streams (e.g., stream
400 sinuosity and bed shape factor) for the D_x models can further reduce the uncertainty in estimation of
401 longitudinal dispersion parameter.

402 Data availability

403 The data used in this study can be obtained from <https://doi.org/10.1007/s11269-018-2139-6>

404 References

- 405 1. Atique, U., Kwon, S. and An, K.G., 2020. Linking weir imprints with riverine water chemistry,
406 microhabitat alterations, fish assemblages, chlorophyll-nutrient dynamics, and ecological health
407 assessments. *Ecological Indicators*, 117, 106652. <https://doi.org/10.1016/j.ecolind.2020.106652>
- 408 2. Kim, J.Y., Atique, U. and An, K.G., 2021. Relative Abundance and Invasion Dynamics of Alien Fish
409 Species Linked to Chemical Conditions, Ecosystem Health, Native Fish Assemblage, and Stream
410 Order. *Water*, 13(2), 158. <https://doi.org/10.3390/w13020158>
- 411 3. Ramezani, M., Noori, R., Hooshyaripor, F., Deng, Z. and Sarang, A., 2019. Numerical modelling-
412 based comparison of longitudinal dispersion coefficient formulas for solute transport in rivers.
413 *Hydrological Sciences Journal*, 64(7), 808-819. <https://doi.org/10.1080/02626667.2019.1605240>
- 414 4. Abolfathi, S., Cook, S., Yeganeh-Bakhtiary, A., Borzooei, S. and Pearson, J. M., 2020. Microplastics
415 transport and mixing mechanisms in the nearshore region. *Coastal Engineering Proceedings 36v*.
416 <https://doi.org/10.9753/icce.v36v.papers.63>
- 417 5. Rutherford, J C. (1994). *River Mixing*. John Wiley & Sons, Chichester, U K, 347 pp.
- 418 6. Abolfathi, S., and Pearson, J. M., 2017. Application of smoothed particle hydrodynamics (SPH) in
419 nearshore mixing: a comparison to laboratory data. *Coastal Engineering Proceedings (35)*.
420 <https://doi.org/10.9753/icce.v35.currents.16>
- 421 7. Cook, S., Chan, H. L., Abolfathi, S., Bending, G. D., Schäfer, H. and Pearson, J. M., 2020.
422 Longitudinal dispersion of microplastics in aquatic flows using fluorometric techniques. *Water*
423 *Research*, 170, 115337. <https://doi.org/10.1016/j.watres.2019.115337>
- 424 8. Cheme, E.K. and Mazaheri, M., 2021. The effect of neglecting spatial variations of the parameters in
425 pollutant transport modeling in rivers. *Environmental Fluid Mechanics*, 21(3), 587-603.
426 <https://doi.org/10.1007/s10652-021-09787-5>
- 427 9. Fischer, H.B., 1967. The mechanics of dispersion in natural streams. *Journal of the Hydraulics*
428 *division*, 93(6), 187-216. <https://doi.org/10.1061/JYCEAJ.0001706>
- 429 10. Fischer, H.B., 1968. Methods for Predicting Dispersion Coefficients in Natural Streams: With
430 Applications to Lower Reaches of the Green and Duwamish Rivers, *Washington* (Vol. 582). US
431 Government Printing Office.
- 432 11. Deng, Z.Q., Bengtsson, L., Singh, V.P. and Adrian, D.D., 2002. Longitudinal dispersion coefficient in
433 single-channel streams. *Journal of Hydraulic Engineering*, 128(10), 901-916.
434 [https://doi.org/10.1061/\(ASCE\)0733-9429\(2002\)128:10\(901\)](https://doi.org/10.1061/(ASCE)0733-9429(2002)128:10(901))
- 435 12. Noori, R., Mirchi, A., Hooshyaripor, F., Bhattarai, R., Haghighi, A.T. and Kløve, B., 2021.
436 Reliability of functional forms for calculation of longitudinal dispersion coefficient in rivers. *Science*
437 *of The Total Environment*, 148394. <https://doi.org/10.1016/j.scitotenv.2021.148394>
- 438 13. Seo, I.W. and Cheong, T.S., 1998. Predicting longitudinal dispersion coefficient in natural streams.
439 *Journal of hydraulic engineering*, 124(1), 25-32. [https://doi.org/10.1061/\(ASCE\)0733-9429\(1998\)124:1\(25\)](https://doi.org/10.1061/(ASCE)0733-9429(1998)124:1(25))
- 440

- 441 14. Nezu, I., Tominaga, A. and Nakagawa, H., 1993. Field measurements of secondary currents in
442 straight rivers. *Journal of Hydraulic Engineering*, 119(5), 598-614.
443 [https://doi.org/10.1061/\(ASCE\)0733-9429\(1993\)119:5\(598\)](https://doi.org/10.1061/(ASCE)0733-9429(1993)119:5(598))
- 444 15. Deng, Z.Q. and Singh, V.P., 1999. Mechanism and conditions for change in channel pattern. *Journal*
445 *of Hydraulic Research*, 37(4), 465-478. <https://doi.org/10.1080/00221686.1999.9628263>
- 446 16. Marion, A. and Zaramella, M., 2006. Effects of velocity gradients and secondary flow on the
447 dispersion of solutes in a meandering channel. *Journal of Hydraulic Engineering*, 132(12), 1295-
448 1302. [https://doi.org/10.1061/\(ASCE\)0733-9429\(2006\)132:12\(1295\)](https://doi.org/10.1061/(ASCE)0733-9429(2006)132:12(1295))
- 449 17. Bashitialshaaer, R., Bengtsson, L., Larson, M., Persson, K.M., Aljaradin, M. and Hossam, A.I., 2011.
450 Sinuosity effects on longitudinal dispersion coefficient. *Int. J. of Sustainable Water and*
451 *Environmental Systems*, 2(2), 77-84.
- 452 18. Nikora, V. and Roy, A.G., 2012. Secondary flows in rivers: Theoretical framework, recent advances,
453 and current challenges. *Gravel bed rivers: Processes, tools, environments*, 3-22.
454 <https://doi.org/10.1002/9781119952497.ch1>
- 455 19. Kişi, Ö., 2009. Modeling monthly evaporation using two different neural computing techniques.
456 *Irrigation Science*, 27(5), 417-430. <https://doi.org/10.1007/s00271-009-0158-z>
- 457 20. Khatibi, R., Ghorbani, M.A., Kashani, M.H. and Kisi, O., 2011. Comparison of three artificial
458 intelligence techniques for discharge routing. *Journal of Hydrology*, 403(3-4), 201-212.
459 <https://doi.org/10.1016/j.jhydrol.2011.03.007>
- 460 21. Abolfathi, S., Yeganeh-Bakhtiary, A., Hamze-Ziabari, S.M., Borzooei, S., 2016. Wave runup
461 prediction using M5' model tree algorithm. *Ocean Engineering*, 112, 76-81.
462 <https://doi.org/10.1016/j.oceaneng.2015.12.016>
- 463 22. Granata, F., Papirio, S., Esposito, G., Gargano, R. and De Marinis, G., 2017. Machine learning
464 algorithms for the forecasting of wastewater quality indicators. *Water*, 9(2), 105.
465 <https://doi.org/10.3390/w9020105>
- 466 23. Jaramillo, F., Orchard, M., Muñoz, C., Antileo, C., Sáez, D. and Espinoza, P., 2018. On-line
467 estimation of the aerobic phase length for partial nitrification processes in SBR based on features
468 extraction and SVM classification. *Chemical Engineering Journal*, 331, 114-123.
469 <https://doi.org/10.1016/j.cej.2017.07.185>
- 470 24. Ahmadi, M.H., Ahmadi, M.A., Nazari, M.A., Mahian, O. and Ghasempour, R., 2019. A proposed
471 model to predict thermal conductivity ratio of Al₂O₃/EG nanofluid by applying least squares support
472 vector machine (LSSVM) and genetic algorithm as a connectionist approach. *Journal of Thermal*
473 *Analysis and Calorimetry*, 135(1), 271-281. <https://doi.org/10.1007/s10973-018-7035-z>
- 474 25. Leottau, D.L., Lobos-Tsunekawa, K., Jaramillo, F. and Ruiz-del-Solar, J., 2019. Accelerating
475 decentralized reinforcement learning of complex individual behaviors. *Engineering Applications of*
476 *Artificial Intelligence*, 85, 243-253. <https://doi.org/10.1016/j.engappai.2019.06.019>
- 477 26. Ghimire, S., Yaseen, Z.M., Farooque, A.A., Deo, R.C., Zhang, J., Tao, X., 2021. Streamflow
478 prediction using an integrated methodology based on convolutional neural network and long short-
479 term memory networks. *Scientific Reports*, 11(1), 17497. <https://doi.org/10.1038/s41598-021-96751-4>
- 480
- 481 27. Moosavi, S.R., Wood, D.A., Ahmadi, M.A. and Choubineh, A., 2019. ANN-based prediction of
482 laboratory-scale performance of CO₂-foam flooding for improving oil recovery. *Natural Resources*
483 *Research*, 28(4), 1619-1637. <https://doi.org/10.1007/s11053-019-09459-8>
- 484 28. Borzooei, S., Miranda, G. H. B., Abolfathi, S., Scibilia, G., Meucci, L., Zanetti, M. C., 2020.
485 Application of unsupervised learning and process simulation for energy optimization of a WWTP
486 under various weather conditions. *Water Science & Technology*, 81(8), 1541-1551.
487 <https://doi.org/10.2166/wst.2020.220>
- 488 29. Yaseen, Z.M., Ali, M., Sharafati, A., Al-Ansari, N., Shahid, S., 2021. Forecasting standardized
489 precipitation index using data intelligence models: regional investigation of Bangladesh. *Scientific*
490 *Reports*, 11(1), 3435. <https://doi.org/10.1038/s41598-021-82977-9>

- 491 30. Afan, H.A., Allawi, M.F., El-Shafie, A., Yaseen, Z.M., Ahmed, A.N., Malek, M.A., Koting, S.B.,
492 Salih, S.Q., Mohtar, W.H.M.W., Lai, S.H. and Sefelnasr, A., 2020. Input attributes optimization using
493 the feasibility of genetic nature inspired algorithm: Application of river flow forecasting. *Scientific*
494 *Reports*, 10(1), 4684. <https://doi.org/10.1038/s41598-020-61355-x>
- 495 31. Tayfur, G. and Singh, V.P., 2005. Predicting longitudinal dispersion coefficient in natural streams by
496 artificial neural network. *Journal of Hydraulic Engineering*, 131(11), 991-1000.
497 [https://doi.org/10.1061/\(ASCE\)0733-9429\(2005\)131:11\(991\)](https://doi.org/10.1061/(ASCE)0733-9429(2005)131:11(991))
- 498 32. Toprak, Z.F., Hamidi, N., Kisi, O. and Gerger, R., 2014. Modeling dimensionless longitudinal
499 dispersion coefficient in natural streams using artificial intelligence methods. *KSCE Journal of Civil*
500 *Engineering*, 18(2), 718-730. <https://doi.org/10.1007/s12205-014-0089-y>
- 501 33. Parsaie, A., Emamgholizadeh, S., Azamathulla, H.M. and Haghiabi, A.H., 2018. ANFIS-based PCA
502 to predict the longitudinal dispersion coefficient in rivers. *International Journal of Hydrology Science*
503 *and Technology*, 8(4), 410-424. <https://doi.org/10.1504/IJHST.2018.095537>
- 504 34. Azar, N.A., Milan, S.G. and Kayhomayoon, Z., 2021. The prediction of longitudinal dispersion
505 coefficient in natural streams using LS-SVM and ANFIS optimized by Harris hawk optimization
506 algorithm. *Journal of Contaminant Hydrology*, 240, 103781.
507 <https://doi.org/10.1016/j.jconhyd.2021.103781>
- 508 35. Di Nunno, F. and Granata, F., 2020. Groundwater level prediction in Apulia region (Southern Italy)
509 using NARX neural network. *Environmental Research*, 190, 110062.
510 <https://doi.org/10.1016/j.envres.2020.110062>
- 511 36. Tayfur, G., 2006. Fuzzy, ANN, and regression models to predict longitudinal dispersion coefficient in
512 natural streams. *Hydrology Research*, 37(2), 143-164. <https://doi.org/10.2166/nh.2006.0012>
- 513 37. Toprak, Z.F. and Cigizoglu, H.K., 2008. Predicting longitudinal dispersion coefficient in natural
514 streams by artificial intelligence methods. *Hydrological Processes: An International Journal*, 22(20),
515 4106-4129. <https://doi.org/10.1002/hyp.7012>
- 516 38. Toprak, Z.F. and Savci, M.E., 2007. Longitudinal dispersion coefficient modeling in natural channels
517 using fuzzy logic. *CLEAN–Soil, Air, Water*, 35(6), 626-637. <https://doi.org/10.1002/clen.200700122>
- 518 39. Piotrowski, A.P., Rowinski, P.M. and Napiorkowski, J.J., 2012. Comparison of evolutionary
519 computation techniques for noise injected neural network training to estimate longitudinal dispersion
520 coefficients in rivers. *Expert Systems with Applications*, 39(1), 1354-1361.
521 <https://doi.org/10.1016/j.eswa.2011.08.016>
- 522 40. Sahay, R.R., 2013. Predicting longitudinal dispersion coefficients in sinuous rivers by genetic
523 algorithm. *Journal of Hydrology and Hydromechanics*, 61(3), 214. <https://doi.org/10.2478/johh-2013-0028>
- 524
- 525 41. Najafzadeh, M. and Tafarjnoruz, A., 2016. Evaluation of neuro-fuzzy GMDH-based particle swarm
526 optimization to predict longitudinal dispersion coefficient in rivers. *Environmental Earth Sciences*,
527 75(2), 157. <https://doi.org/10.1007/s12665-015-4877-6>
- 528 42. Noori, R., Ghiasi, B., Sheikhan, H. and Adamowski, J.F., 2017. Estimation of the dispersion
529 coefficient in natural rivers using a granular computing model. *Journal of Hydraulic Engineering*,
530 143(5), 04017001. [https://doi.org/10.1061/\(ASCE\)HY.1943-7900.0001276](https://doi.org/10.1061/(ASCE)HY.1943-7900.0001276)
- 531 43. Kargar, K., Samadianfard, S., Parsa, J., Nabipour, N., Shamshirband, S., Mosavi, A. and Chau, K.W.,
532 2020. Estimating longitudinal dispersion coefficient in natural streams using empirical models and
533 machine learning algorithms. *Engineering Applications of Computational Fluid Mechanics*, 14(1),
534 311-322. <https://doi.org/10.1080/19942060.2020.1712260>
- 535 44. Riahi-Madvar, H., Dehghani, M., Parmar, K.S., Nabipour, N. and Shamshirband, S., 2020.
536 Improvements in the explicit estimation of pollutant dispersion coefficient in rivers by subset
537 selection of maximum dissimilarity hybridized with ANFIS-firefly algorithm (FFA). *IEEE Access*, 8,
538 60314-60337. <https://doi.org/10.1109/ACCESS.2020.2979927>
- 539 45. Noori, R., Deng, Z., Kiaghadi, A. and Kachooangi, F.T., 2016. How reliable are ANN, ANFIS, and
540 SVM techniques for predicting longitudinal dispersion coefficient in natural rivers?. *Journal of*
541 *Hydraulic Engineering*, 142(1), 04015039. [https://doi.org/10.1061/\(ASCE\)HY.1943-7900.0001062](https://doi.org/10.1061/(ASCE)HY.1943-7900.0001062)

- 542 46. Ghiasi, B., Sheikhan, H., Zeynolabedin, A. and Niksokhan, M.H., 2019. Granular computing–neural
543 network model for prediction of longitudinal dispersion coefficients in rivers. *Water Science and*
544 *Technology*, 80(10), 1880-1892. <https://doi.org/10.2166/wst.2020.006>
- 545 47. Sheikhan, H., Delavar, M.R. and Stein, A., 2017. A GIS-based multi-criteria seismic vulnerability
546 assessment using the integration of granular computing rule extraction and artificial neural networks.
547 *Transactions in GIS*, 21(6), 1237-1259. <https://doi.org/10.1111/tgis.12274>
- 548 48. Yao, Y., 2004. A partition model of granular computing. In *Transactions on rough sets I* (232-253).
549 *Springer*, Berlin, Heidelberg. https://doi.org/10.1007/978-3-540-27794-1_11
- 550 49. Sheikhan, H., Delavar, M.R. and Stein, A., 2015. Integrated estimation of seismic physical
551 vulnerability of Tehran using rule based granular computing. *The International Archives of*
552 *Photogrammetry, Remote Sensing and Spatial Information Sciences*, 40(3), 187.
553 <https://doi.org/10.5194/isprsarchives-XL-3-W3-187-2015>
- 554 50. Khamespanah, F., Delavar, M.R., Moradi, M. and Sheikhan, H., 2016. A GIS-based multi-criteria
555 evaluation framework for uncertainty reduction in earthquake disaster management using granular
556 computing. *Geodesy and Cartography*, 42(2), 58-68. <https://doi.org/10.3846/20296991.2016.1199139>
- 557 51. Deng, Z.Q., Singh, V.P. and Bengtsson, L., 2001. Longitudinal dispersion coefficient in straight
558 rivers. *Journal of hydraulic engineering*, 127(11), 919-927. [https://doi.org/10.1061/\(ASCE\)0733-9429\(2001\)127:11\(919\)](https://doi.org/10.1061/(ASCE)0733-9429(2001)127:11(919))
- 560 52. Barati Moghaddam, M., Mazaheri, M. and MohammadVali Samani, J., 2017. A comprehensive one-
561 dimensional numerical model for solute transport in rivers. *Hydrology and Earth System Sciences*,
562 21(1), 99-116. <https://doi.org/10.5194/hess-21-99-2017>
- 563 53. Kilpatrick, F.A. and Wilson, J.F., 1989. Measurement of time of travel in streams by dye tracing (Vol.
564 3). *US Government Printing Office*.
- 565 54. Iwasa, Y. and Aya, S., 1991. Transverse mixing in a river with complicated channel geometry.
566 *Bulletin of the Disaster Prevention Research Institute*, 41(3), 129-175.
- 567 55. Liu, H., 1977. Predicting dispersion coefficient of streams. *Journal of the Environmental Engineering*
568 *Division*, 103(1), 59-69. <https://doi.org/10.1061/JEEGAV.0000605>
- 569 56. Smith, R., 1992. 'Physics of Dispersion' coastal and estuarine pollution – methods and solutions'
570 technical sessions, *Scottish hydraulic study group*, One day seminar 3rd April, Glasgow.
- 571 57. Taylor, G.I., 1954. The dispersion of matter in turbulent flow through a pipe. *Proceedings of the*
572 *Royal Society of London. Series A. Mathematical and Physical Sciences*, 223(1155), 446-468.
573 <https://doi.org/10.1098/rspa.1954.0130>
- 574 58. Taylor, G.I., 1953. Dispersion of soluble matter in solvent flowing slowly through a tube.
575 *Proceedings of the Royal Society of London. Series A. Mathematical and Physical Sciences*,
576 219(1137), 186-203. <https://doi.org/10.1098/rspa.1953.0139>
- 577 59. Elder, J., 1959. The dispersion of marked fluid in turbulent shear flow. *Journal of fluid mechanics*,
578 5(4), 544-560. <https://doi.org/10.1017/S0022112059000374>
- 579 60. Fischer, H.B., 1966. Longitudinal dispersion in laboratory and natural streams. *California Institute of*
580 *Technology*. <https://doi.org/10.7907/Z9F769HC>
- 581 61. Carr, M.L. and Rehmann, C.R., 2007. Measuring the dispersion coefficient with acoustic Doppler
582 current profilers. *Journal of Hydraulic Engineering*, 133(8), 977-982.
583 [https://doi.org/10.1061/\(ASCE\)0733-9429\(2007\)133:8\(977\)](https://doi.org/10.1061/(ASCE)0733-9429(2007)133:8(977))
- 584 62. Papadimitrakis, I. and Orphanos, I., 2004. Longitudinal dispersion characteristics of rivers and natural
585 streams in Greece. *Water, Air and Soil Pollution: Focus*, 4(4), 289-305.
586 <https://doi.org/10.1023/B:WAFO.0000044806.98243.97>
- 587 63. Fischer, H.B., List, J.E., Koh, C.R., Imberger, J. and Brooks, N.H., 1979. Mixing in inland and
588 coastal waters. *Academic press*, New York.
- 589 64. Riahi-Madvar, H., Dehghani, M., Seifi, A. and Singh, V.P., 2019. Pareto optimal multigene genetic
590 programming for prediction of longitudinal dispersion coefficient. *Water resources management*,
591 33(3), 905-921. <https://doi.org/10.1007/s11269-018-2139-6>

- 592 65. Yao, Y.Y., 2001, October. On modeling data mining with granular computing. In *25th Annual*
593 *International Computer Software and Applications Conference. COMPSAC 2001* (638-643). IEEE.
594 <https://doi.org/10.1109/CMPSAC.2001.960680>
- 595 66. Yao, J.T. and Yao, Y.Y., 2002, October. Induction of classification rules by granular computing. In
596 *International Conference on Rough Sets and Current Trends in Computing* (331-338). Springer,
597 Berlin, Heidelberg. https://doi.org/10.1007/3-540-45813-1_43
- 598 67. Yao, Y.Y. and Zhong, N., 2002. Granular computing using information tables. *Data mining, rough*
599 *sets and granular computing*, 102-124. https://doi.org/10.1007/978-3-7908-1791-1_5
- 600 68. Efron, B. and Tibshirani, R.J., 1994. An introduction to the bootstrap. *CRC press*.
- 601 69. Srivastav, R.K., Sudheer, K.P. and Chaubey, I., 2007. A simplified approach to quantifying predictive
602 and parametric uncertainty in artificial neural network hydrologic models. *Water Resources Research*,
603 43(10). <https://doi.org/10.1029/2006WR005352>
- 604 70. Abbaspour, K.C., Yang, J., Maximov, I., Siber, R., Bogner, K., Mieleitner, J., Zobrist, J. and
605 Srinivasan, R., 2007. Modelling hydrology and water quality in the pre-alpine/alpine Thur watershed
606 using SWAT. *Journal of Hydrology*, 333(2-4), 413-430. <https://doi.org/10.1016/j.jhydrol.2006.09.014>
- 607 71. Bello, R., Falcón, R. and Pedrycz, W. eds., 2007. Granular computing: at the junction of rough sets
608 and fuzzy sets (Vol. 224). *Springer*.
- 609 72. Koh, Y.S. and Rountree, N. eds., 2009. Rare Association Rule Mining and Knowledge Discovery:
610 Technologies for Infrequent and Critical Event Detection: Technologies for Infrequent and Critical
611 Event Detection (Vol. 3). *IGI Global*.
- 612 73. Etemad-Shahidi, A. and Taghipour, M., 2012. Predicting longitudinal dispersion coefficient in natural
613 streams using M5' model tree. *Journal of hydraulic engineering*, 138(6), 542-554.
614 [https://doi.org/10.1061/\(ASCE\)HY.1943-7900.0000550](https://doi.org/10.1061/(ASCE)HY.1943-7900.0000550)
- 615 74. Sahay, R.R. and Dutta, S., 2009. Prediction of longitudinal dispersion coefficients in natural rivers
616 using genetic algorithm. *Hydrology Research*, 40(6), 544-552. <https://doi.org/10.2166/nh.2009.014>
- 617 75. Najafzadeh, M., Noori, R., Afroozi, D., Ghiasi, B., Hosseini-Moghari, S.M., Mirchi, A., Haghghi,
618 A.T. and Kløve, B., 2021. A comprehensive uncertainty analysis of model-estimated longitudinal and
619 lateral dispersion coefficients in open channels. *Journal of Hydrology*, 126850.
620 <https://doi.org/10.1016/j.jhydrol.2021.126850>
- 621 76. Ghiasi, B., Jodeiri, A. and Andik, B., 2021. Using a deep convolutional network to predict the
622 longitudinal dispersion coefficient. *Journal of Contaminant Hydrology*. 240, 103798.
623 <https://doi.org/10.1016/j.jconhyd.2021.103798>
- 624 77. Sahay, R.R., 2011. Prediction of longitudinal dispersion coefficients in natural rivers using artificial
625 neural network. *Environmental Fluid Mechanics*, 11(3), 247-261. <https://doi.org/10.1007/s10652-010-9175-y>
- 626 78. Adarsh, S., 2010. Prediction of longitudinal dispersion coefficient in natural channels using soft
627 computing techniques. *Scientia Iranica*, 17(5), 363-371.
- 628 79. Noori, R., Karbassi, A., Farokhnia, A. and Dehghani, M., 2009. Predicting the longitudinal dispersion
629 coefficient using support vector machine and adaptive neuro-fuzzy inference system techniques.
630 *Environmental Engineering Science*, 26(10), 1503-1510. <https://doi.org/10.1089/ees.2008.0360>
- 631 80. Memarzadeh, R., Zadeh, H.G., Dehghani, M., Riahi-Madvar, H., Seifi, A., Mortazavi, S.M., 2020. A
632 novel equation for longitudinal dispersion coefficient prediction based on the hybrid of SSMD and
633 whale optimization algorithm. *Science of The Total Environment*, 716, 137007.
634 <https://doi.org/10.1016/j.scitotenv.2020.137007>
- 635 81. Dehghani, M., Zargar, M., Riahi-Madvar, H., Memarzadeh, R., 2020. A novel approach for
636 longitudinal dispersion coefficient estimation via tri-variate archimedean copulas. *Journal of*
637 *Hydrology*, 584, 124662. <https://doi.org/10.1016/j.jhydrol.2020.124662>
- 638
639

640

641 **Competing interests**

642 The authors declare that they have no known competing financial interests or personal relationships that
643 could have appeared to influence the work reported in this paper.

644 **Author contributions**

645 Data collection and analysis were carried out by **B.G., S.U., H.S.** and **A.Z. R.N.** conceived the study
646 conceptually. The models were ran by **R.N.** and **H.S.** The first draft of manuscript was prepared by **B.G.,**
647 **R.N., S.U., C.J.** and **M.H.** The funding acquisition was made by **C.J.** and **M.H.** The analyses and results
648 were supervised and validated by **R.N., S.M.B.** and **S.A.** All authors read and approved the final version
649 of manuscript.

650